THz generation from water wedge excited by dual-color pulse

Min Li (李 敏)[1], Zhenyu Li (李振宇)[1], Junyi Nan (南君义)[2], Yu Xia (夏 宇)[1], Mingyang He (贺明洋)[1], Feng Wang (王 锋)[1], Wenhui Lu (卢文晖)[1], Shuai Yuan (袁 帅)[2], and Heping Zeng (曾和平)[1,2,*]

[1]*Shanghai Key Laboratory of Modern Optical System, Engineering Research Center of Optical Instrument and System, Ministry of Education, School of Optical-Electrical and Computer Engineering, University of Shanghai for Science and Technology, Shanghai 200093, China*

[2]*State Key Laboratory of Precision Spectroscopy, East China Normal University, Shanghai 200062, China*

**Corresponding author: hpzeng@phy.ecnu.edu.cn*

Received February 18, 2020; accepted April 30, 2020; posted online June 8, 2020

Terahertz (THz) waves could be generated through exciting a gravity-guided, free-flowing water wedge by a dual-color pulse. It is not required to rotate the optimal angle considering the water film as an ionization medium. It is demonstrated to be more effective to generate stronger THz radiation when the ionization position is on the front surface of the air water interface of the water wedge by moving its position. The effect of pulse energy on THz generation is also investigated, and it is observed that with the increase of pulse energy the THz electric field shows a quadratic rising trend. These observations are consistent with air plasma induced THz emission.

Keywords: water wedge; THz; plasma.
doi: 10.3788/COL202018.073201.

Compared with traditional light sources, terahertz (THz) pulsed light sources have important development prospects in industrial applications, military, medical, and biological fields[1–5]. For a long period of time, researchers focused on high-efficiency THz emission sources[6–11]. Laser induced plasma is gradually becoming the preferred solution for THz generation due to impressive intensity and a remarkably wide spectrum, as well as no damage threshold limitation[10,12–16]. Water has not been used as an ionized medium for a long time due to its strong absorption for THz, although it has lower ionization energy and higher molecular density than air[17–20]. Counterintuitive observation has certified that THz radiation could be detected from ultrashort pulse induced plasma in liquids, which showed a higher magnitude than that obtained from laser induced plasma in air[21]. Subsequently, monochromatic laser irradiated gravity-guided, free-flowing water film with thickness of about 200 μm and liquid-water line with a diameter of about 200 μm were both demonstrated to produce a stronger THz electric field, respectively[22–24]. Furthermore, the THz electric field increased 10 times, while the dual-color pulse was replaced to excite water film at 50 fs pulse duration[25]. It is noteworthy that the water film with thickness of 170–200 μm driven by gravity breaks down at pulse energy of 0.4 mJ, which significantly limits further enhancement of THz emission[22]. A water jet and thin water column driven by fixed pressure can bear higher laser power, more than 2 mJ[23,26–28]. But, the water jet needs to be designed with great precision, and it can only meet the requirements of a certain fixed thickness of water film. The fixed pressure driven thin water column can just provide a fixed flow rate, and it is difficult to keep the shape of water at longer distances. Therefore, it is imperative to explore the mechanism of THz generation from water and innovative methods to generate THz wave.

In this Letter, a water wedge acts as the ionized medium excited by dual-color pulses, which forms through gravity driven water flowing along a thin plate with width of 1 mm and aluminum wire due to the surface tension of water. This device has been shown to bear higher laser intensity than water film and has advantages of stable structure and flexible parameter. It is experimentally demonstrated that even stronger THz emission could be produced after ionizing the water wedge than water film excited by dual-color laser pulse at 0° incident angle. The phenomenon is attributed to the net current both from asymmetric dual-color electric field and non-uniform distribution of plasma excited by transverse laser intensity in the laser incident plane. The THz electric field at different pulse energy is also investigated to further analyze the dependence of THz electric field on plasma density, which proves that the mechanism of THz generation from dual-color pulse induced water plasma is similar to that produced by air plasma.

Figure 1 shows a schematic diagram of our experiment. The laser pulse was delivered from a Ti:sapphire amplifier with a central wavelength 800 nm, pulse duration of 60 fs, repetition rate of 1 kHz, and horizontal polarization. The pump pulse with adjustable energy from 0.2 to 1.4 mJ passed through a 0.3-mm-thick beat barium borate (β-BBO) crystal to generate dual-color pulses with orthogonal polarization. Subsequently, a 0.1-mm-thick alpha barium borate (α-BBO) crystal was used to compensate for optical path difference of dual-color pulses. Both polarizations of the dual-color pulse were controlled to

 © 2020 Chinese Optics Letters

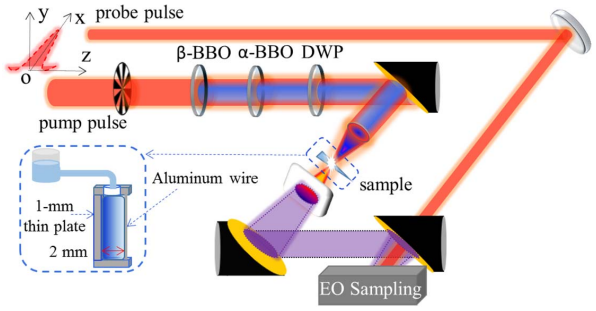

Fig. 1. Experimental setup. The laser pulse travels along the z axis. The β-BBO crystal with 0.3 mm thickness is used to generate dual-color pulse, a 0.1-mm-thick α-BBO crystal is applied to compensate the phase delay of the dual-color pulse, and a 0.04-mm-thick DWP is a dual-wavelength plate. The "sample" is the water wedge. EO Sampling, the electro-optical detection. Inset: schematic diagram of water wedge generation, a 1-mm-wide thin plate is on the left, and an aluminum wire is on the right. The surface asymmetry of the water wedge is changed by changing the diameter of the aluminum wires.

vertical polarization by a 0.04-mm-thick dual-wave plate (DWP, half-wave plate for 800 nm and full-wave plate for 400 nm). Collinear-propagation dual-color pulses focused by a parabolic mirror with a 2 in. effective focal length were employed to irradiate a sub-millimeter water wedge formed by gravity. A pair of parabolic mirrors were placed to collect forward THz emission from water plasma and converged in an electric optical (EO) sampling device with another weak probe pulse. A 4-mm-thick Teflon plate and a 300-μm-thick high-resistance silicon were placed after water plasma to eliminate the residual pump pulse. The illustration in Fig. 1 shows formation of the sub-millimeter water wedge. The relative distance between a 1 mm thin plate and aluminum wire was fixed to 2 mm. Moreover, the width of the right side was adjustable by replacing aluminum wires of different diameters. A water wedge formed as water flowed freely.

As shown in Fig. 2(a), the experiment result has shown that a weak THz electric field could be generated through exciting water film by dual-color pulse at 0° incident angle, and the THz electric field derived by water plasma from a water wedge with a 200 μm wire is about two times

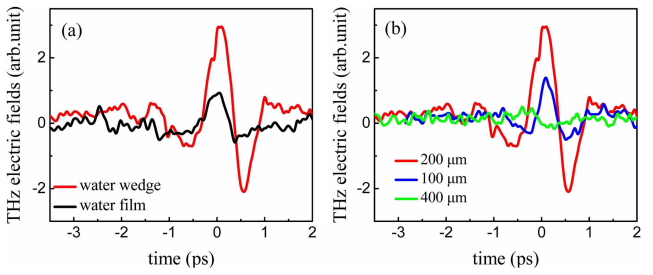

Fig. 2. (a) THz electric fields generated from the water film (black solid line) and the water wedge (red solid line). (b) Comparison of THz electric fields obtained from the water wedge produced by aluminum wires with different diameters.

larger than that obtained from water film at the same dual-color pulse energy of 1 mJ. The water film device consists of two aluminum wires with a diameter of 200 μm, and the flow rate of water is 20 mL/min. The water flow rate in the water wedge is controlled at 50 mL/min, and the laser incident position is located at the center position in the x-axis direction of the structure. The phenomenon is analyzed from the perspective of physical mechanism and water plasma distribution. According to the model of Sacchi[29] and Kennedy[30], we can assume that water is an amorphous semiconductor with a bandwidth of 6.5 eV[18]. This indicates that the multiphoton ionization theory can be applied to water at this time, and the formation of plasma in water can be regarded as the formation of electron-hole pairs. The ionized free electrons are accelerated in a laser field plane until the end of the laser field. Each electron absorbs multiple photons from the field and independently ionizes. Different from the water film in the single-color field, which uses ponderomotive force to drive the free electrons generated by ionization, a non-zero transverse plasma current formed in the wake of the symmetry-broken laser field, resulting in the initial THz emission. In addition, the current is affected, as the preformed THz electric field interacted with the plasma. Therefore, the net current is the combining effect of the above two processes. Plasma is accelerated in an asymmetric electric field of an asymmetric water structure. By changing the diameters of the wires, the THz radiation generated by the three different surface symmetry water wedges is shown in Fig. 2(b). Non-uniform plasma density distribution enhanced the net current and effectively promoted THz emission. That is why the water wedge could generate a stronger THz electric field than the water film in Fig. 2(a). However, the slope of the water wedge has intensity not the only factor affecting THz. The electric field of THz generation from the structure with a 200 μm wire has intensity two times that with a 100 μm wire, the signal strength is still stronger than that produced by the water film at 0°, and the signal strength is almost invisible with a 400 μm wire. The 100 μm wire is so thin that plasma cannot be kept in water, although it increases the slope of the water wedge, while most THz is absorbed at 400 μm, and it reduces the slope of the laser when it enters the water wedge. The subsequent relationship between the ionization position of the plasma and the THz electric field also indirectly verified this result.

To further understand the mechanism of THz generation from water plasma, the water wedge was moved along the laser transmission direction. Amplitudes of THz electric field from water plasma along with different positions are displayed in Fig. 3(a). The position at which the THz waveform could be generated was defined as zero, and positive distances indicated an opposite direction to the z axis, as shown in Fig. 1. As seen in Fig. 3(a), the THz electric field increased dramatically while the water wedge moved backward along the z axis, in which process the ionization focus moves toward the front surface of the water wedge. The spectra with different spectral widths

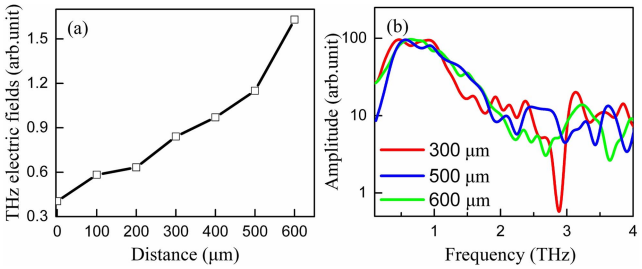

Fig. 3. (a) The detected THz electric fields from the water wedge as a function of the distance the water moves. (The position after moving 600 μm is where the laser focus is closest to the front surface when THz can be detected.) (b) The detected THz spectra after moving 300 μm, 500 μm, and 600 μm.

at 300 μm, 500 μm, and 600 μm are compared in Fig. 3(b). According to the photocurrent model, the non-zero transverse plasma is determined by

$$J = eN_e v, \tag{1}$$

where e is electron charge, N_e is electron density, and v is the velocity of electron movement. It has been proved repeatedly that the first interface of air–water played a major role in THz generation from water plasma in this Letter. As the water wedge moved backward, the density of ionized electrons produced by the first interface increased due to the increase of the dual-color laser field, resulting in the partial increase of the THz electric field. At the same time, the closer the laser focus is to the first interface, the greater the spatial distribution asymmetry of dual-color laser intensity at the first interface plane. Both the enhancement of the asymmetric electric field and the spatial asymmetry of plasma density at the first interface together increase the net current. Therefore, the THz electric field increased significantly while it was closer to the first interface, as shown in Fig. 3(a). Meanwhile, the spectral width widened, and the central frequency slightly shifted. It is well known that water generally produces plasma with better uniformity and shorter length, although the THz generation provided by the dual-color field plays a role in the initial stage, the THz generated from the interaction of plasma and the initial THz electric field dominates after the rapid excitation of the plasma; moreover, the plasma resonance angular frequency determines the central frequency of the generated THz electric field. Assuming uniformly distributed plasma in a cylinder volume and neglecting the absorption of the plasma, the electric field distribution in the cylindrical plasma can be simplified to

$$E = -\frac{a}{1+\epsilon} E_{\text{int}}, \tag{2}$$

where $\epsilon = 1 - (\frac{\omega_p}{\omega})^2$ is the plasma dielectric constant, E_{int} is the initial broadband THz electric field generated from the dual-color field through the photocurrent mechanism, and a is a constant. The central frequency of the THz pulse is as follows:

$$f_{\text{THz}} = \omega_{\text{res}}/2\pi = k\omega_p/2\pi, \tag{3}$$

where ω_{res} is the plasma resonance angular frequency ($\omega_{\text{res}} = k\omega_p$), k is a constant depending on the geometry of the plasma, and $\omega_p = \sqrt{e^2 N_e/m_e\epsilon_0}$ (N_e is the electronic density, this change in spectrum is not just a single frequency change in ω_p, and it appears as a reduction in the width of a frequency domain; m_e is the electronic quality, and ϵ_0 is the vacuum dielectric constant)[31]. Obviously, the central frequency moves to higher frequencies as the plasma density increases. The spectral width decreases as the center frequency decreases as well.

To confirm the dependence of the THz electric field on the dual-color pulse energy, the dual-color pulse energy grows monotonically from 0.2 mJ to 1.4 mJ. Figure 4 shows the dependence of the THz electric field on the dual-color pulse energy, in which a quadratic increase is observed. Since the laser has a strong self-focusing effect in water, we set the radius of the focal spot of the laser in the water to 25 μm; then, the laser intensity in the energy range of 0.2–1.4 mJ is from $2.04 \times 10^{14}\,\text{W}\cdot\text{cm}^{-2}$ to $1.42 \times 10^{15}\,\text{W}\cdot\text{cm}^{-2}$. The laser intensity required for the second-order ionization of oxygen is above $2 \times 10^{15}\,\text{W}\cdot\text{cm}^{-2}$ of the laser intensity required for the second-order ionization of nitrogen, and hydrogen and oxygen have first-order complete ionization energies of almost equal size. In such a laser intensity range, the first-order ionization of hydrogen and oxygen has completely occurred, and the second-order ionization of oxygen is weak but has been increasing. During this process, the multiphoton ionization rate is proportional to I^k, where I is the laser intensity, and $k = \langle \frac{\Delta E}{\hbar\omega} + 1 \rangle$ ($\langle\rangle$ represents rounding); it means that in order to ionize an atom or molecule whose ionization energy is ΔE, k photons are required. It is clearly visible that with the linear increase

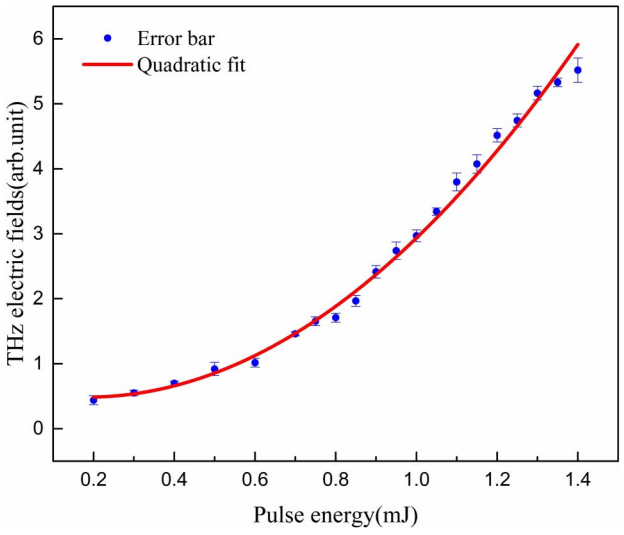

Fig. 4. The detected THz electric fields from the water wedge as a function of the total excitation laser pulse (ω and 2ω) energy. (Blue, the error bar of nine measurements. Red, the quadratic fitting line.)

of I, the plasma ionization rate increases rapidly[32]. According to the THz generation process from ionized air plasma, $|E_{\mathrm{THz}}| \propto A(\varphi)\omega_p$, where $A(\varphi) \propto I^{1/2}$ is the vector potential, and $\omega_p \propto N_e^{1/2}$ is the plasma resonance frequency[33]. According to the equation, the rapid increase of N_e and the linear increase of I result in a quadratic growth in the THz electric field, which is consistent with the trend shown in Fig. 4. Considering the asymmetry of the water wedge, the slight enhancement is caused by the ionization position moving from pulse peak to the pulse rising edge as the laser intensity increases, which results in slightly different electron density of the first-order completed ionization. The trend of the THz electric field along with the pulse energy reveals a similar phenomenon with THz generation from air plasma, and the THz electric field is mainly determined by electron density. The results help us better understand the physical mechanism of THz generation produced by the ionization of water.

In summary, we realize the THz generation through innovative use of a water wedge as the ionizing medium. These experimental results strongly verified that the THz electric field from water plasma is affected by plasma density, plasma spatial distribution, and pulse energy, and further confirm water could be used as an effective medium to generate strong THz pulses. The trend of the THz electric field along with pulse energy reveals the critical role of plasma density in THz generation process. Fortunately, it provides an effective method for strong THz generation and far-field THz application.

This work was supported by the National Natural Science Foundation of China (Nos. 11727812 and 61927813) and the National Key Research and Development Program of China (No. 2018YFB0504400).

References

1. F. M. Al-Douseri, Y. Chen, and X. C. Zhang, Int. J. Infrared Millimeter Waves **27**, 481 (2006).
2. R. A. Cheville and D. Grischkowsky, Appl. Phys. Lett. **67**, 1960 (1995).
3. M. Ortolani, J. S. Lee, U. Schade, and H. W. Hübers, Appl. Phys. Lett. **93**, 081906 (2008).
4. H. Hoshina, A. Hayashi, N. Miyoshi, F. Miyamaru, and C. Otani, Appl. Phys. Lett. **94**, 123901 (2009).
5. S. M. Kim, F. Hatami, J. S. Harris, A. W. Kurian, J. Ford, D. King, G. Scalari, M. Giovannini, N. Hoyler, J. Faist, and G. Harris, Appl. Phys. Lett. **88**, 153903 (2006).
6. R. A. Lewis, J. Phys. D: Appl. Phys. **47**, 374001 (2014).
7. D. R. Dykaar, B. I. Greene, J. F. Federici, A. F. J. Levi, L. N. Pfeiffer, and R. F. Kopf, Appl. Phys. Lett. **59**, 262 (1991).
8. M. Reid, I. V. Cravetchi, R. Fedosejevs, I. M. Tiginyanu, and L. Sirbu, Appl. Phys. Lett. **86**, 021904 (2005).
9. J. H. Booske, R. J. Dobbs, C. D. Joye, C. L. Kory, G. R. Neil, G. S. Park, J. Park, and R. J. Temkin, IEEE Trans. Terahertz Sci. Technol. **1**, 54 (2011).
10. Y. Minami, T. Kurihara, K. Yamaguchi, M. Nakajima, and T. Suemoto, Appl. Phys. Lett. **102**, 041105 (2013).
11. C. Vicario, M. Jazbinsek, A. V. Ovchinnikov, O. V. Chefonov, S. I. Ashitkov, M. B. Agranat, and C. P. Hauri, Opt. Express **23**, 4573 (2015).
12. K. Y. Kim, J. H. Glownia, A. J. Taylor, and G. Rodriguez, Opt. Express **15**, 4577 (2007).
13. K. Y. Kim, A. J. Taylor, J. H. Glownia, and G. Rodriguez, Nat. Photon. **2**, 605 (2008).
14. J. Dai, N. Karpowicz, and X. C. Zhang, Phys. Rev. Lett. **103**, 0203001 (2009).
15. A. D. Koulouklidis, C. Gollner, V. Shumakova, V. Y. Fedorov, A. Pugžlys, A. Baltuška, and S. Tzortzakis, Nat. Commun. **11**, 292 (2020).
16. K. Kang, L. L. Zhang, T. Wu, K. Li, and C. L. Zhang, Chin. Opt. Lett. **11**, 110401 (2018).
17. C. J. Ruan, D. Y. Kong, J. Dai, K. L. Chen, S. J. Guo, and X. J. Wu, Chin. Opt. Lett. **7**, 073001 (2019).
18. F. Williams, S. P. Varma, and S. Hillenius, J. Chem. Phys. **64**, 1549 (1976).
19. D. N. Nikogosyan, A. A. Oraevsky, and V. I. Rupasov, Chem. Phys. **77**, 131 (1983).
20. R. A. Crowell and D. M. Bartels, J. Phys. Chem. **100**, 17940 (1996).
21. I. Dey, K. Jana, V. Y. Fedorov, A. D. Koulouklidis, A. Mondal, M. Shaikh, D. Sarkar, A. D. Lad, S. Tzortzakis, A. Couairon, and G. R. Kumar, Nat. Commun. **8**, 1184 (2017).
22. Q. Jin, Y. W. E, K. Williams, J. Dai, and X. C. Zhang, Appl. Phys. Lett. **111**, 071103 (2017).
23. L. L. Zhang, W. M. Wang, T. Wu, S. J. Feng, K. Kang, C. L. Zhang, Y. Zhang, Y. T. Li, Z. M. Sheng, and X. C. Zhang, Phys. Rev. Appl. **12**, 014005 (2019).
24. Y. W. E, Q. Jin, and X. C. Zhang, Appl. Phys. Lett. **115**, 101101 (2019).
25. Q. Jin, J. Dai, Y. W. E, and X. C. Zhang, Appl. Phys. Lett. **113**, 261101 (2018).
26. H. Huang, T. Nagashima, W. Hsu, S. Juodkazis, and K. Hatanaka, Nanomaterials **8**, 523 (2018).
27. Y. W. E, Q. Jin, A. Tcypkin, and X. C. Zhang, Appl. Phys. Lett. **113**, 181103 (2018).
28. S. J. Feng, L. Q. Dong, T. Wu, Y. Tan, R. Zhang, L. L. Zhang, C. L. Zhang, and Y. J. Zhao, Chin. Opt. Lett. **18**, 023202 (2020).
29. P. K. Kennedy, D. X. Hammer, and B. A. Rockwell, Prog. Quantum Electron. **21**, 155 (1997).
30. C. A. Sacchi, J. Opt. Soc. Am. B **8**, 337 (1991).
31. N. Li, Y. Bai, T. S. Miao, P. Liu, R. X. Li, and Z. Z. Xu, Phys. Opt. **1601**, 07974 (2016).
32. J. Noack and A. Vogel, J. IEEE Quantum. Electron. **35**, 1156 (1999).
33. W.-M. Wang, Y.-T. Li, Z.-M. Sheng, X. Lu, and J. Zhang, Phys. Rev. E **87**, 033108 (2013).